

**Temperature-responsive copolymers without compositional drift by RAFT
copolymerization of 2-(acryloyloxy)ethyl trimethylammonium chloride and 2-
(diethylamino) ethyl acrylate**

Sofia Rodrigues^{1,2,3}, Marie-Thérèse Charreyre*^{2,3}, Arnaud Favier^{2,3}, Carlos Baleizão¹,
José Paulo S. Farinha*¹

¹ *Centro de Química Estrutural (CQE) and Institute of Nanoscience and Nanotechnology (IN), Instituto Superior Técnico, University of Lisbon, Lisboa, Portugal.*

² *Univ Lyon, ENS de Lyon, CNRS USR 3010, Laboratoire Joliot-Curie (LJC), F-69364 Lyon, France.*

³ *Univ Lyon, INSA-Lyon, CNRS UMR 5223, Laboratoire Ingénierie des Matériaux Polymères (IMP), F-69621 Villeurbanne, France.*

Electronic Supplementary Information

1. Size Exclusion Chromatography (SEC)	2
2. Solubility	3
3. Determination of monomer conversion	4
4. Free radical polymerization kinetics	10
5. RAFT polymerization	13
6. Evolution of feed molar composition with conversion	19
7. (co)Polymer NMR spectra	20
8. (co)Polymer molecular weights	21
9. References	23

1. Size Exclusion Chromatography (SEC)

Aqueous SEC was performed in acetate buffer eluent (acetic acid 0.2 mol L⁻¹ and ammonium acetate 0.15 mol L⁻¹, pH 4.5), at a flow rate of 0.8 mL min⁻¹, 23 °C) using a Shimadzu Prominence system consisting of a LC-20AD peristaltic pump, a DGU-20A3R degassing unit, and a Rheodyne 7725i injector (injection volume of 20 µL). Three detectors in series were used: a Shimadzu Prominence RF-20A fluorimetric detector, a multi-angle static light-scattering (MALS) Wyatt MiniDawn Treos detector, and a Waters 2410 Refractive Index detector (internal temperature 40 °C). Data acquisition and analysis were made with Astra 5.3.2.1 software from Wyatt.

The chromatography columns were either:

- two Waters Ultrahydrogel Linear WAT011545 analytical columns of 300 mm length and 7.8 mm internal diameter, connected in series, with a Phenomenex KJ0-4282 guard cartridge system.
- three columns in series: 2 linear (same as in previous case) and a TSKgel G3000PW (MW<50000 g mol⁻¹), with the same as above guard cartridge system.
- same conditions as in previous case, but with eluent at 10 °C (instead of 23 °C) and without guard cartridge system.
- two TSKgel columns: a G2500PW (MW<3000 g mol⁻¹) and a G6000PW (MW<8x10⁶ g mol⁻¹).

The columns were in a Shimadzu Prominence CTO-20AC column oven (40 °C). Analyses were performed by injection of 100 µL of polymer solution (approx. 0.5 mg mL⁻¹) in the acetate buffer previously filtered through a 0.2 µm CME filter.

The molecular weight determination of the homo- and copolymers by SEC-MALS was not possible since we could not obtain chromatograms with size separation.

2. Solubility

Table S1. Monomer and CTA solubility in different solvents.

	DEAEA	AEtMACl	CPADB
H₂O	y	y	y ^a
EtOH	y	y	y
DMSO	y	y	y
1,4-dioxane	y	emulsion	y
CDCl₃	y	n	y
DMF	y	n	y
Acetone	y	y ^a	y
Diethyl ether	y	two phases	y
n-pentane	y	two phases	y

y = soluble; n = not soluble.

^aSoluble when previously dissolved in some drops of ethanol.

Table S2. (co)polymer solubility in different solvents for precipitation assays.

	PDEAEA	PDEAEA ⁺	PAEtMACl	P(AEtMACl-co-DEAEA ⁺)
Diethyl ether	y	n	+/-	n
CHCl₃	y	#	+/-	#
Acetone	y	y	n	+/-
THF	y	#	#	n
n-Pentane	y	+/-	#	#
Dioxane	y	y ^a	n	n
H₂O	y	y	y	y
DMF	#	y	n	n

y = soluble; n = not soluble; +/- = partially soluble; # = not determined.

^aSoluble after stirring all night.

3. Determination of monomer conversion

¹H NMR method 1, based on an internal standard, for experiments carried out below 80°C.

Method 1 is based on the addition of an internal standard (trioxane, 5.1 ppm in CDCl₃) to the polymerization¹ to quantify the decrease of DEAEA or AEtMACl vinyl proton resonances (Figure S1). The monomer conversion after time t , $p_{Mon}(t)$, is given by Eq. S1 where H_{Mon} is the integral value of the three vinyl protons of DEAEA or AEtMACl monomer and H_{Triox} is the integral value of the trioxane protons.

$$p_{Mon}(t) = 1 - \frac{\left(\frac{H_{Mon}}{H_{Triox}}\right)_t}{\left(\frac{H_{Mon}}{H_{Triox}}\right)_{t=0}} \quad (\text{Eq. S1})$$

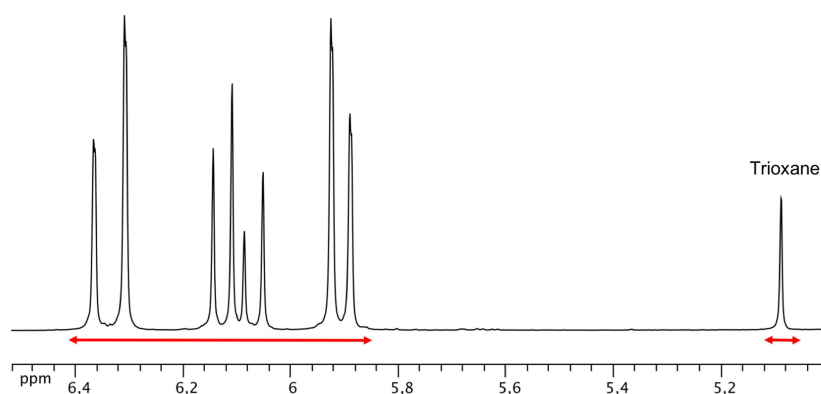


Figure S1. Enlarged part (3 vinylic protons and trioxane peak) of the ¹H NMR spectrum (D₂O) of the polymerization medium during AEtMACl homopolymerization (Exp. 6, t₀), indicating the considered zones (red arrows) to determine conversion using trioxane as internal standard (NMR method 1).

This method provided the best accuracy (below 2%) and reproducibility for experiments carried out below 80°C. When temperature was higher than the solvent boiling point (78°C for ethanol under 760 mmHg), we noticed that the accuracy decreased probably because of the co-evaporation of some trioxane.

¹H NMR method 2, for AEtMAcI homopolymerization above 80°C.

Method 2 is based on the comparison between the ¹H NMR resonances of residual monomer² and growing polymer chain (backbone part). Four zones were identified as A, B, C and D (Figure S2) and the proton assignment led to Eq. S2, where H_{Mon} is the integral value of one proton of AEtMAcI monomer, H_{Poly} is the integral value of one proton of PAEtMAcI homopolymer and $p_{AEtMAcI}(t)$ is the AEtMAcI conversion at time t . The (D/3)/(A/2) ratio was the most reliable (compared to the other ones) since among the four zones, A and D were the most clearly defined. A very good accuracy (around 2%) was obtained for conversions above 20%, with a sufficiently high signal/noise ratio for the polymer backbone resonances.

$$\left\{ \begin{array}{l} A \propto 2H_{Poly} + 2H_{Mon} \\ B \propto 2H_{Poly} + 2H_{Mon} \\ C \propto 9H_{Poly} + 9H_{Mon} \\ D \propto 3H_{Poly} \end{array} \right. \Rightarrow p_{AEtMAcI}(t) = \frac{H_{Poly}}{H_{Mon} + H_{Poly}} = \frac{D/3}{A/2} = \frac{D/3}{B/2} = \frac{D/3}{C/9} \quad (\text{Eq. S2})$$

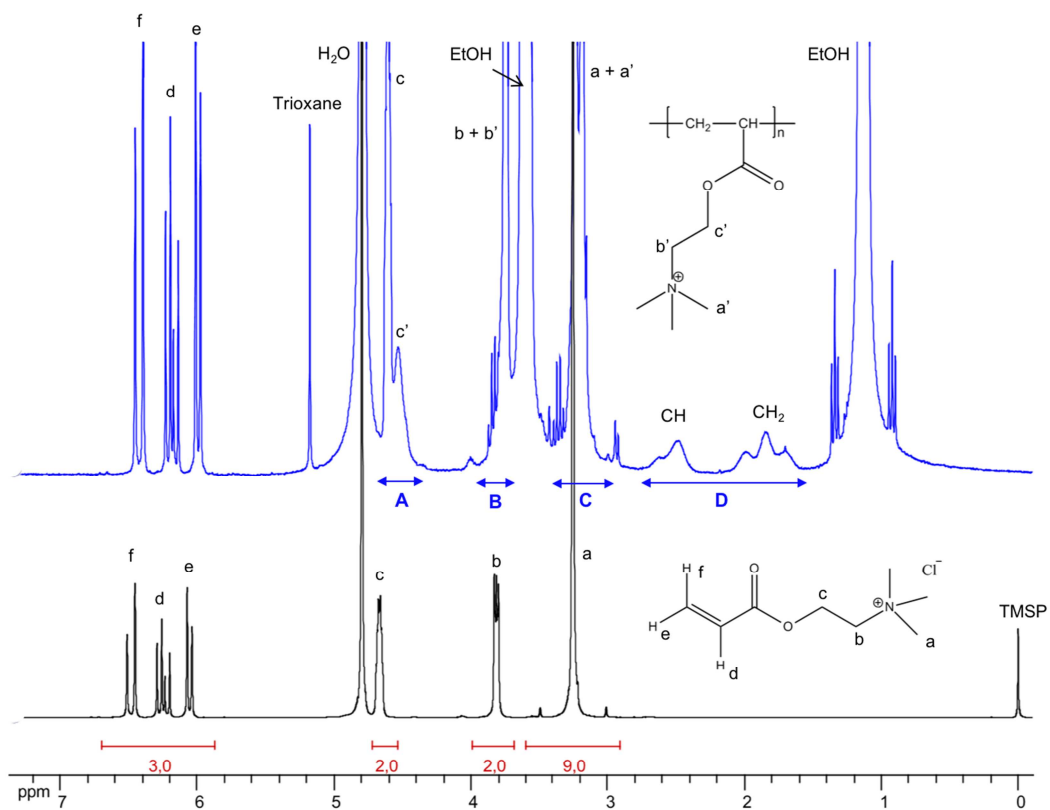


Figure S2. ^1H NMR spectrum in D_2O of (bottom) AEtMACl monomer and (top) the reaction medium during AEtMACl RAFT homopolymerization (Exp. 8, t_4 , 30% conversion), with the different zones (A, B, C, D) used to determine the conversion.

¹H NMR method 3, for DEAEA homopolymerization above 80°C.

Method 3 is based on a given proton of DEAEA (noted d, Figure S3) for which the corresponding ¹H NMR resonances in residual monomer and polymer are close but clearly resolved (here, the two resonances at 4.44 ppm and 4.2-4.4 ppm, A_{Mon} and A_{Poly}, respectively). Proton assignment led to Eq. S3, where H_{Mon} is the integral value of one proton of DEAEA monomer, H_{Poly} is the integral value of one proton of PDEAEA homopolymer and $p_{DEAEA}(t)$ is DEAEA conversion at time t . With Method 3, a very good accuracy (around 2%) was obtained for conversions as low as 10%, since the considered A_{Poly} resonance at 4.2-4.4 ppm is much narrower than the polymer backbone resonances (between 1.4 and 2.5 ppm) and thus exhibits a better signal/noise ratio. For DEAEA, Method 3 gave better reproducibility than Method 2. For AEtMACl, Method 3 could not be applied since there was no zone where monomer and polymer resonances did not overlap.

$$A_{Mon} \propto 2 H_{Mon}$$

$$A_{Poly} \propto 2 H_{Poly}$$

$$p_{DEAEA}(t) = \frac{H_{Poly}}{H_{Mon} + H_{Poly}} = A_{Poly} / (A_{Mon} + A_{Poly}) \quad (\text{Eq. S3})$$

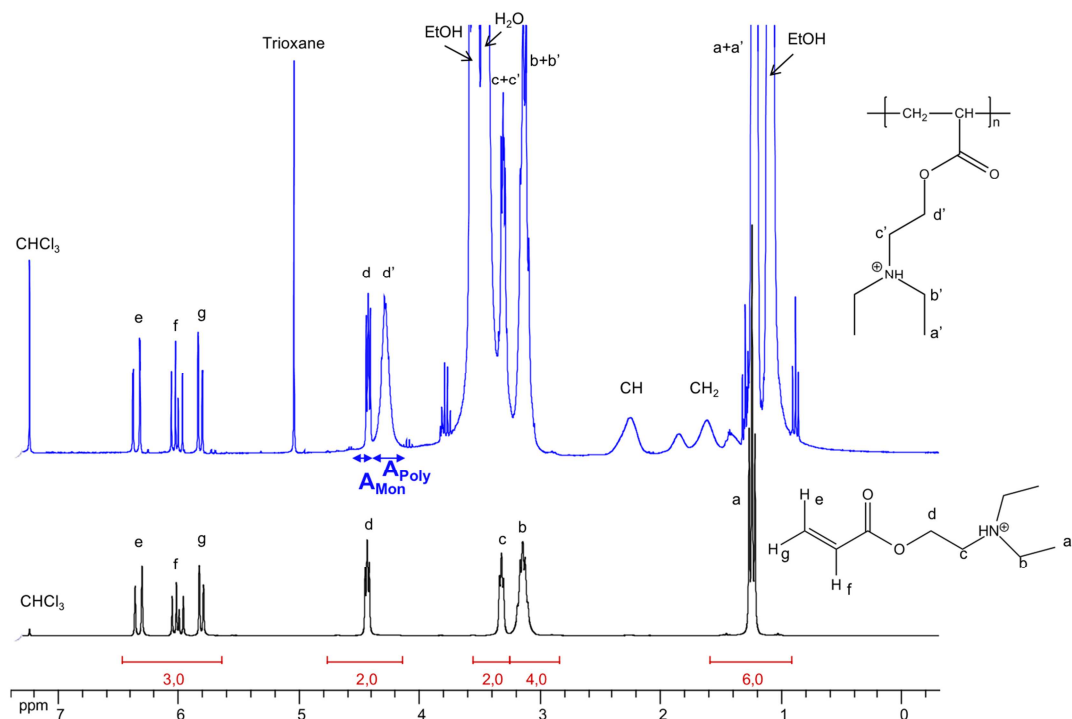


Figure S3. ^1H NMR spectrum in CDCl_3 of (bottom) DEAEA $^+$ monomer and (top) the reaction medium during DEAEA $^+$ RAFT homopolymerization (Exp. 11, t_5 , 29% conversion), with the different zones (A_{Mon} and A_{Poly}) used to determine the conversion.

¹H NMR method 4, for AEtMACI/DEAEA copolymerization.

Method 4 is based on the comparison between the ¹H NMR resonances of residual monomers and growing copolymer backbone. Among the different zones (Eq. S4, Figure S4), combination of zones B and E was the most reliable to determine the global conversion (rather than B and F zones, located on either side of the solvent peak). A very good accuracy (around 2%) was obtained for conversions above 20%, with a sufficiently high signal/noise ratio for the copolymer backbone resonances.

$$\begin{cases} A \propto 6(P_{DEAEA} + M_{DEAEA}) \\ B \propto 3(P_{AEtMACI} + P_{DEAEA}) \\ C \propto 4(P_{DEAEA} + M_{DEAEA}) + 9(P_{AEtMACI} + M_{AEtMACI}) \\ D \propto 2(P_{AEtMACI} + M_{AEtMACI}) \\ E \propto 2(P_{AEtMACI} + M_{AEtMACI}) + 2(P_{DEAEA} + M_{DEAEA}) \\ F \propto 3(M_{AEtMACI} + M_{DEAEA}) \end{cases} \Rightarrow$$

$$\text{Global conv. (t)} = \frac{P_{AEtMACI} + P_{DEAEA}}{((P_{AEtMACI} + P_{DEAEA}) + (M_{AEtMACI} + M_{DEAEA}))} =$$

$$= \frac{B/3}{E/2} = \frac{B/3}{((B/3) + (F/3))} \quad (\text{Eq. S4})$$

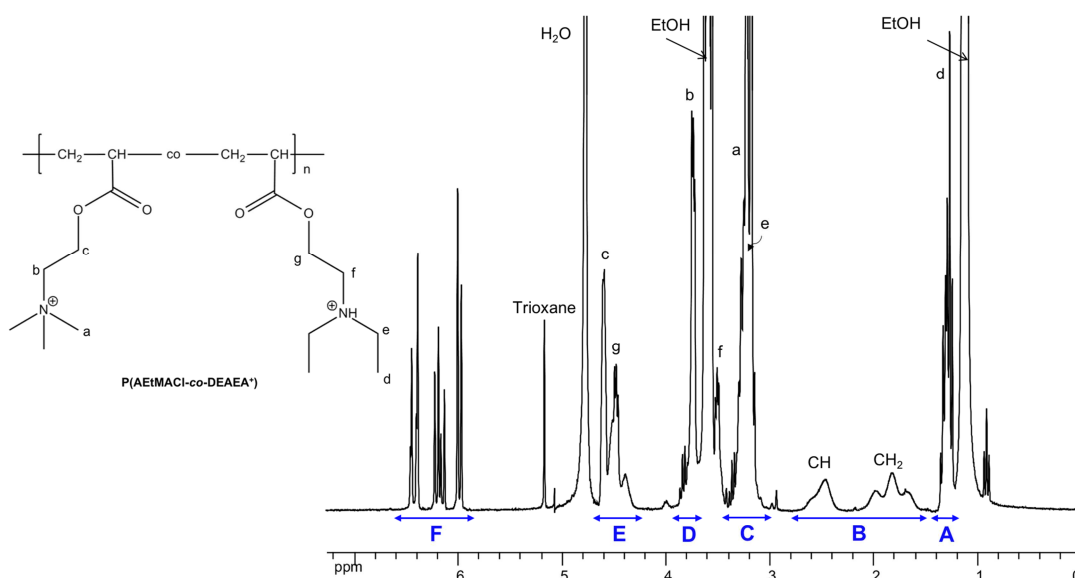


Figure S4. ¹H NMR spectrum in D₂O of the reaction medium during AEtMACI/DEAEA⁺ RAFT copolymerization (Exp. 17, t_s, 44% global conversion), with the different zones (A, B, C, D, E, F) used to determine the conversion.

4. Free radical polymerization kinetics

Several free radical polymerization (FRP) experiments were carried out in usual conditions (Exp. 1 to 4, Table 1 and Figure S5). Monomer, initiator (AIBN), solvent (ethanol) and trioxane (reference for ^1H NMR determination of monomer consumption) were introduced in a Schlenk tube equipped with a magnetic stirrer. The mixture was purged with nitrogen (N_2) and heated in a thermostated oil bath. Periodically, samples were withdrawn from the polymerization medium via a cannula for analyses.

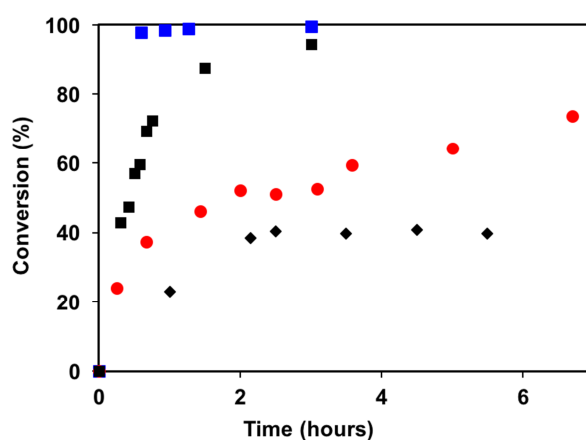


Figure S5. Monomer conversion versus time plots for free radical homopolymerization of DEAEA in ethanol ($[\text{M}]_0=2\text{ M}$ and $[\text{AIBN}]_0=0.02\text{ M}$) at $60\text{ }^\circ\text{C}$ (Exp. 1, ◆) and $70\text{ }^\circ\text{C}$ (Exp. 2, ●), and of AEtMAcI in ethanol at $60\text{ }^\circ\text{C}$ in the same conditions (Exp. 3, $[\text{M}]_0=2\text{ M}$ and $[\text{AIBN}]_0=0.02\text{ M}$, ■) or with different initial monomer and initiator concentrations (Exp. 4, $[\text{M}]_0=1\text{ M}$ and $[\text{AIBN}]_0=0.005\text{ M}$, ■). Conversions were determined by ^1H NMR using Method 1.

In usual conditions (1 mol% initiator compared to monomer), the kinetics of DEAEA free radical polymerization in ethanol at $60\text{ }^\circ\text{C}$ (Exp. 1) reached a plateau at about 40% conversion, that could be increased to 70% conversion at $70\text{ }^\circ\text{C}$ (Exp. 2). A higher plateau was indeed expected according to the homopolymerization rate (R_p , Eq. S5), since higher temperatures induce an increase in the concentration of initiator primary radicals, $[I]$, as well as of all the rate constants, with an order 1 for the propagation rate constant, k_p , compared to an order 0.5 for the termination rate constant, k_t :

$$R_p = -\frac{d[M]}{dt} = k_p [M] \left(\frac{2 \cdot f \cdot [I]}{k_t} \right)^{1/2} \quad (\text{Eq. S5})$$

with

$$[I] = [I]_0 \cdot e^{-k_d \cdot t} \quad (\text{Eq. S6})$$

where $[M]$ and $[I]$ are respectively the monomer and initiator molar concentrations at time t , $[I]_0$ is the initial initiator concentration, f is the initiator efficiency, and k_d is the initiator decomposition rate constant at the considered temperature.

The comparison with homopolymerization of AEtMACl at 60 °C in the same conditions (Exp. 3) indicated a much faster consumption of AEtMACl than of DEAEA. Such behavior reflects a higher reactivity of AEtMACl radicals, as generally observed for charged monomers compared to neutral monomers.³ Even after decreasing monomer concentration and $[I]_0/[M]_0$ ratio to half (Exp. 4), the kinetics of AEtMACl homopolymerization were still faster. It was possible to reach almost 100% AEtMACl conversion within 3 hours.

From the kinetics of DEAEA and AEtMACl homopolymerizations (Exp. 1 and 4, respectively), it was possible to determine the corresponding $k_p/k_t^{1/2}$ ratios by combining Eq. S5 with Eq. S6:⁴

$$-\frac{d[M]}{[M]} = k_p \left(\frac{2 \cdot f \cdot [I]_0}{k_t} \right)^{1/2} e^{-\frac{k_d \cdot t}{2}} dt \quad (\text{Eq. S7})$$

and after integration

$$\ln \left(\frac{[M]_0}{[M]_t} \right) = 2 \frac{k_p}{k_t^{1/2}} \left(\frac{2 \cdot f \cdot [I]_0}{k_d} \right)^{1/2} \left(1 - e^{-\frac{k_d \cdot t}{2}} \right) \quad (\text{Eq. S8})$$

From the slope of the plot $\ln([M]_0/[M]_t)$ versus $(1 - \exp(-k_d t/2))$ (Figure S6), and considering $f = 0.5$ ⁴ and $k_d = 1.53 \times 10^{-5} \text{ s}^{-1}$ for AIBN in ethanol at 60 °C,⁵ we determined $k_p/k_t^{1/2} = 0.09 \text{ L}^{1/2} \text{ mol}^{-1/2} \text{ s}^{-1/2}$ and $1.86 \text{ L}^{1/2} \text{ mol}^{-1/2} \text{ s}^{-1/2}$, respectively, for DEAEA and AEtMACl homopolymerization in ethanol at 60 °C, confirming a higher polymerization rate for AEtMACl than for DEAEA.

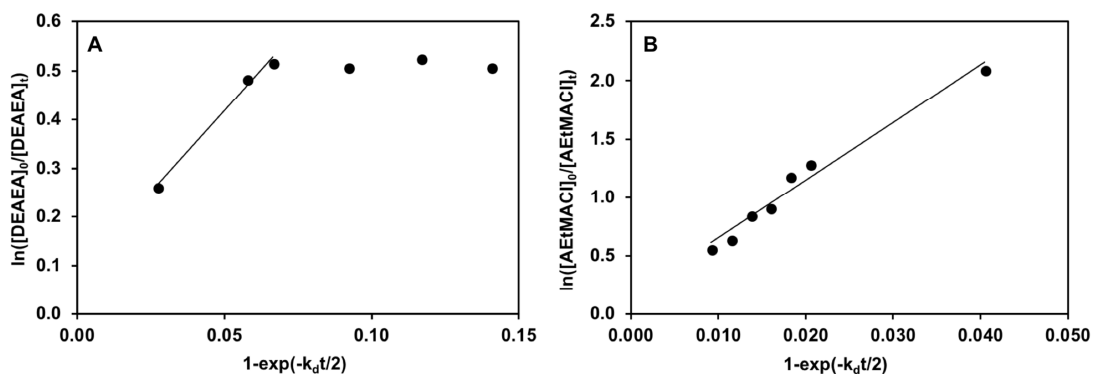


Figure S6. Semi-logarithmic variation of (A) DEAEA conversion (Exp. 1) ($\ln([DEAEA]_0/[DEAEA]_t) = 6.695 (1 - \exp(-\frac{k_d t}{2})) + 0.0836$, $R^2 = 0.989$) and (B) AEtMACl conversion (Exp. 4) ($\ln([AEtMACl]_0/[AEtMACl]_t) = 67.228 (1 - \exp(-\frac{k_d t}{2})) - 0.090$, $R^2 = 0.974$), versus the decomposition rate of initiator according to Eq. S8. For (A), the obtained value is only indicative since it is based on the first three points only.

5. RAFT polymerization

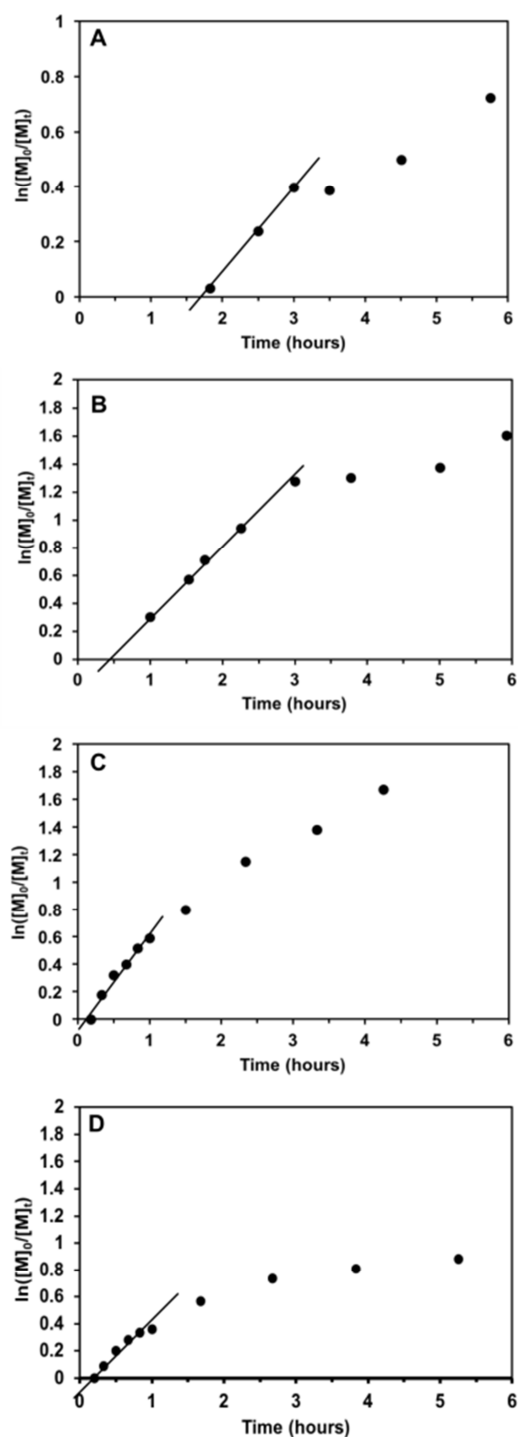


Figure S7. $\ln([M]_0/[M]_t)$ versus time plots for RAFT homopolymerizations: **(A)** AEtMAl homopolymerization, Exp. 5 at 70 °C; **(B)** AEtMAl homopolymerization, Exp. 6 at 80 °C; **(C)** AEtMAl homopolymerization, Exp. 7 at 85 °C, and **(D)** DEAEA⁺ homopolymerization, Exp. 13 at 80 °C. In experiments (B) and (D), respectively corresponding to AEtMAl and DEAEA⁺ homopolymerization at the same temperature and CTA/initiator ratio, the slopes are similar (0.487).

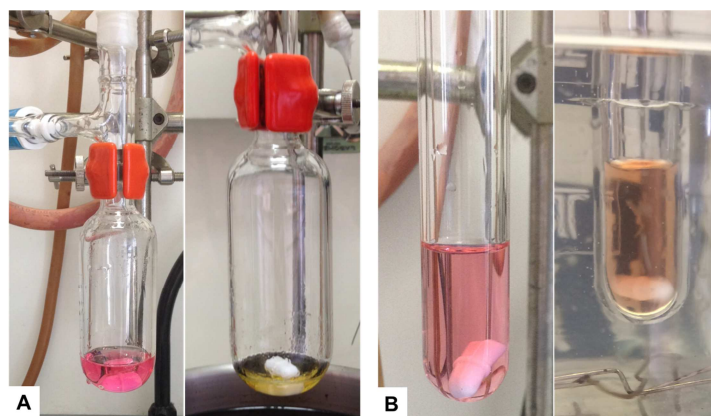


Figure S8. Color change of the reaction medium during the RAFT homopolymerization of DEAEA, from pink (color of the CTA solution in ethanol) to pale yellow (**A**, Exp.9) and of DEAEA⁺, from pink to salmon (**B**, Exp. 11).

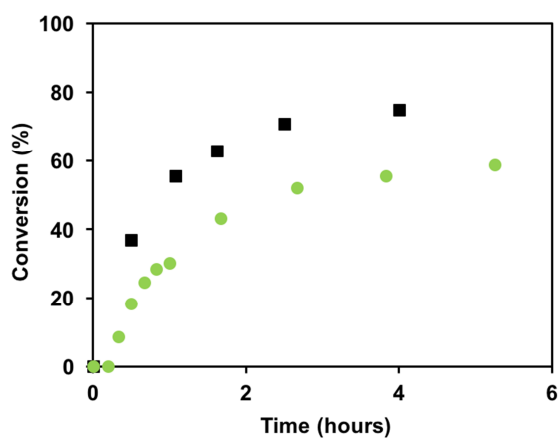


Figure S9. Monomer conversion versus time plots for RAFT homopolymerization of DEAEA⁺ in ethanol at 80°C, targeting longer chains in the same conditions except the [DEAEA⁺]₀/[CTA]₀ ratio, from 217 (Exp. 11, ■) to 388 (Exp. 13, ●). Conversions were determined by ¹H NMR using Method 3.

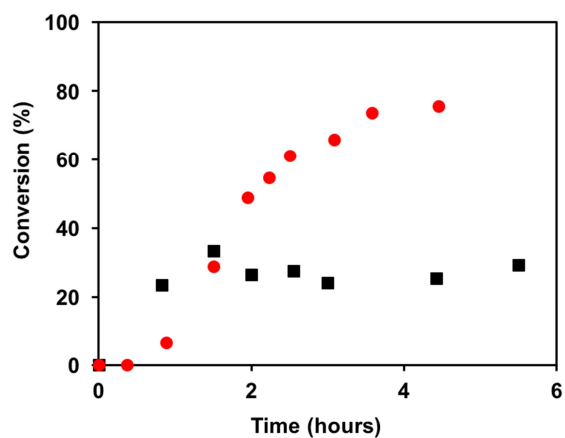


Figure S10. Global monomer conversion versus time plots for AEtMACl/DEAEA 75/25 copolymerization in ethanol at 80 °C, without TFA (Exp. 14, ■) and with TFA (1.2 eq., Exp. 15, ●). Conversions were determined by ^1H NMR using Method 1 (Exp. 14) and Method 4 (Exp. 15).

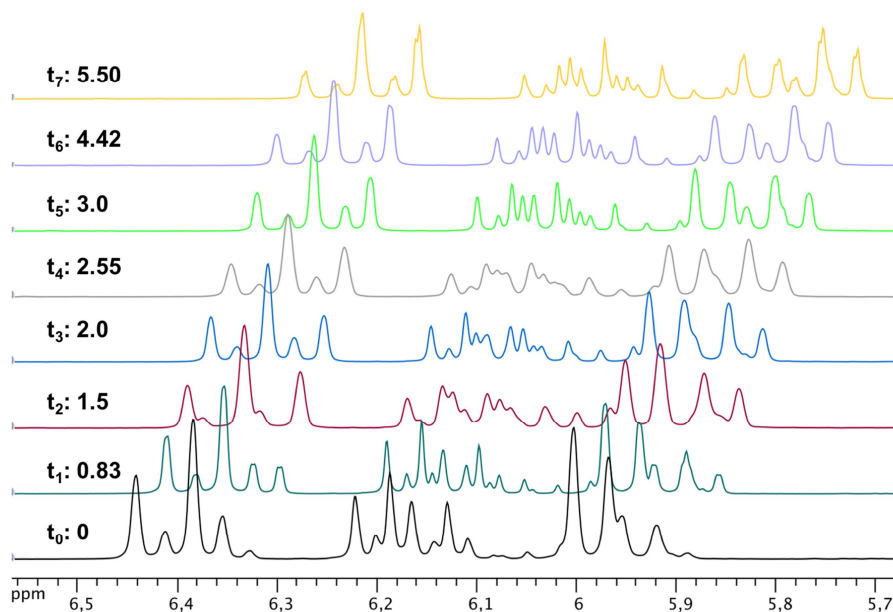


Figure S11. Vinylic region of the ^1H NMR spectra during AEtMACl/DEAEA copolymerization, without TFA (75/25 molar ratio, Exp. 14). Times (t_x) in hours.

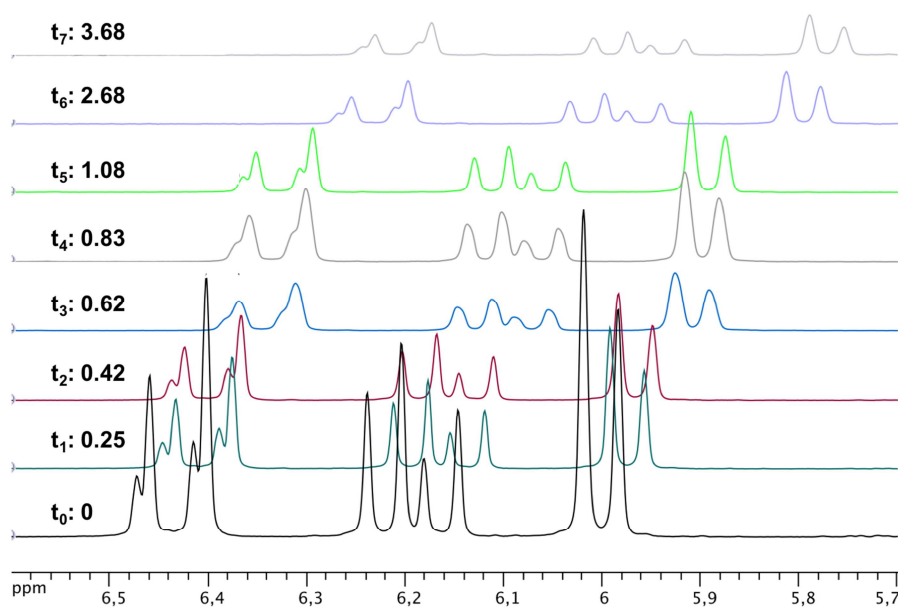


Figure S12. Vinylic region of the ^1H NMR spectra during AEtMACl/DEAEA $^+$ copolymerization, with TFA (75/25 molar ratio, Exp. 17). Times (t_x) in hours.

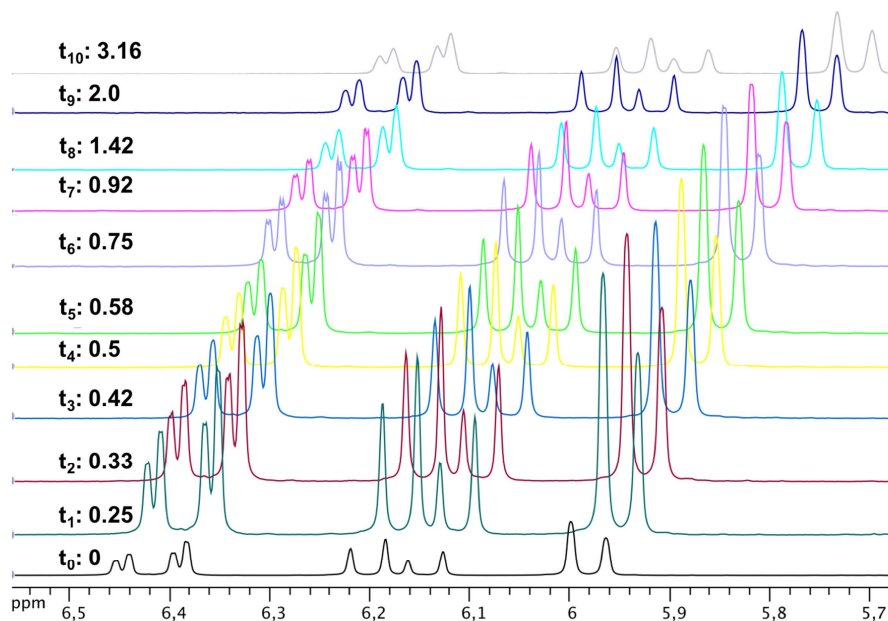


Figure S13. Vinylic region of the ^1H NMR spectra during AEtMACI/DEAEA $^+$ copolymerization, with TFA (60/40 molar ratio, Exp. 18). Times (t_x) in hours.

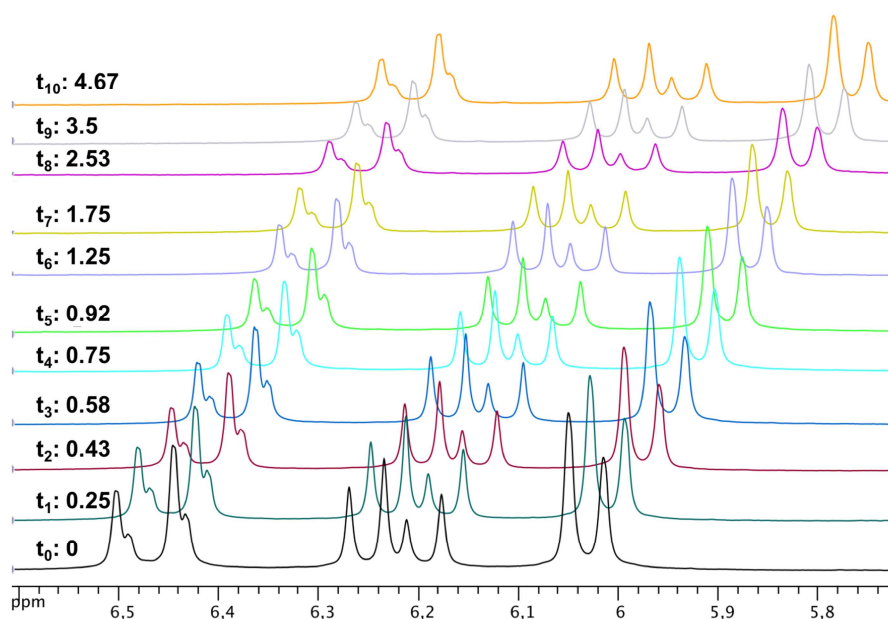


Figure S14. Vinylic region of the ^1H NMR spectra during AEtMACI/DEAEA $^+$ copolymerization, with TFA (25/75 molar ratio, Exp. 19). Times (t_x) in hours.

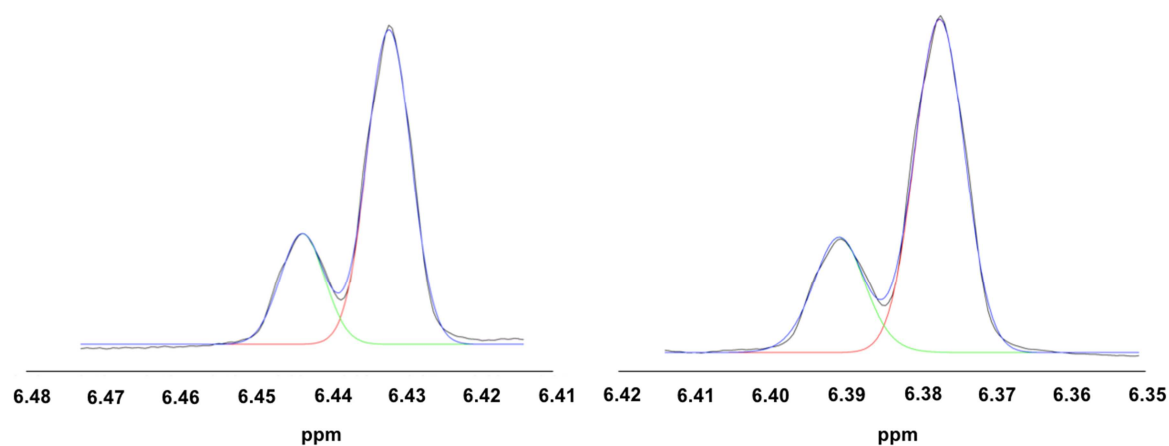


Figure S15. Deconvolution of the original ^1H NMR peaks during copolymerization (Exp. 17, t_1 at time 0.25 h). Original peaks (black line), AEtMACl fit peak (red line), DEAEA $^+$ fit peak (green line) and cumulative fit peak (blue line). The deconvolution was performed with Origin software, using a nonlinear curve fit with a PearsonVII model.

6. Evolution of feed molar composition with conversion

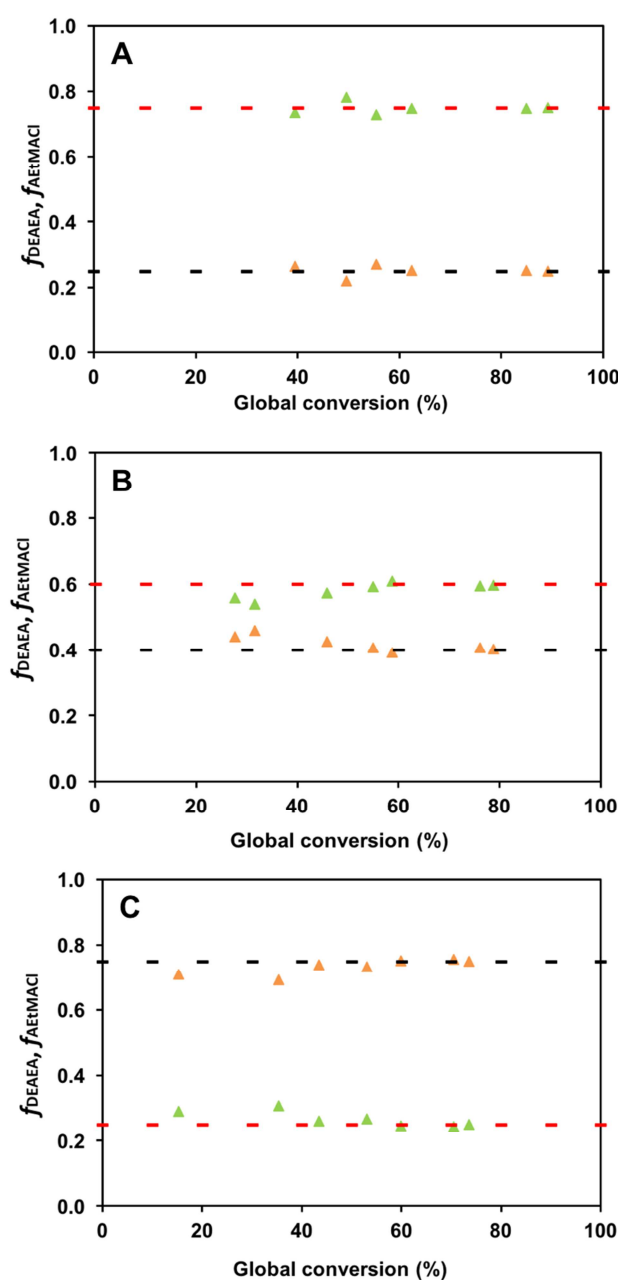


Figure S16. Feed molar composition expressed as molar fractions f_{AEtMACl} (\blacktriangle) (Eq. S9) and f_{DEAEA} (\blacktriangle) (Eq. S10), versus global conversion (initial feed molar composition in AEtMACl (-) and DEAEA⁺ (-)) for AEtMACl/DEAEA⁺ copolymerization using different molar ratios, (A) 75/25 (Exp.17), (B) 60/40 (Exp. 18), and (C) 25/75 (Exp. 19).

$$f_{\text{AEtMACl}} = \frac{[\text{AEtMACl}]_0 \times (1 - p_{\text{AEtMACl}})}{[\text{AEtMACl}]_0 \times (1 - p_{\text{AEtMACl}}) + [\text{DEAEA}]_0 \times (1 - p_{\text{DEAEA}}} \quad (\text{Eq. S9})$$

$$f_{\text{DEAEA}} = \frac{[\text{DEAEA}]_0 \times (1 - p_{\text{DEAEA}})}{[\text{AEtMACl}]_0 \times (1 - p_{\text{AEtMACl}}) + [\text{DEAEA}]_0 \times (1 - p_{\text{DEAEA}}} \quad (\text{Eq. S10})$$

7. (co)Polymer NMR spectra

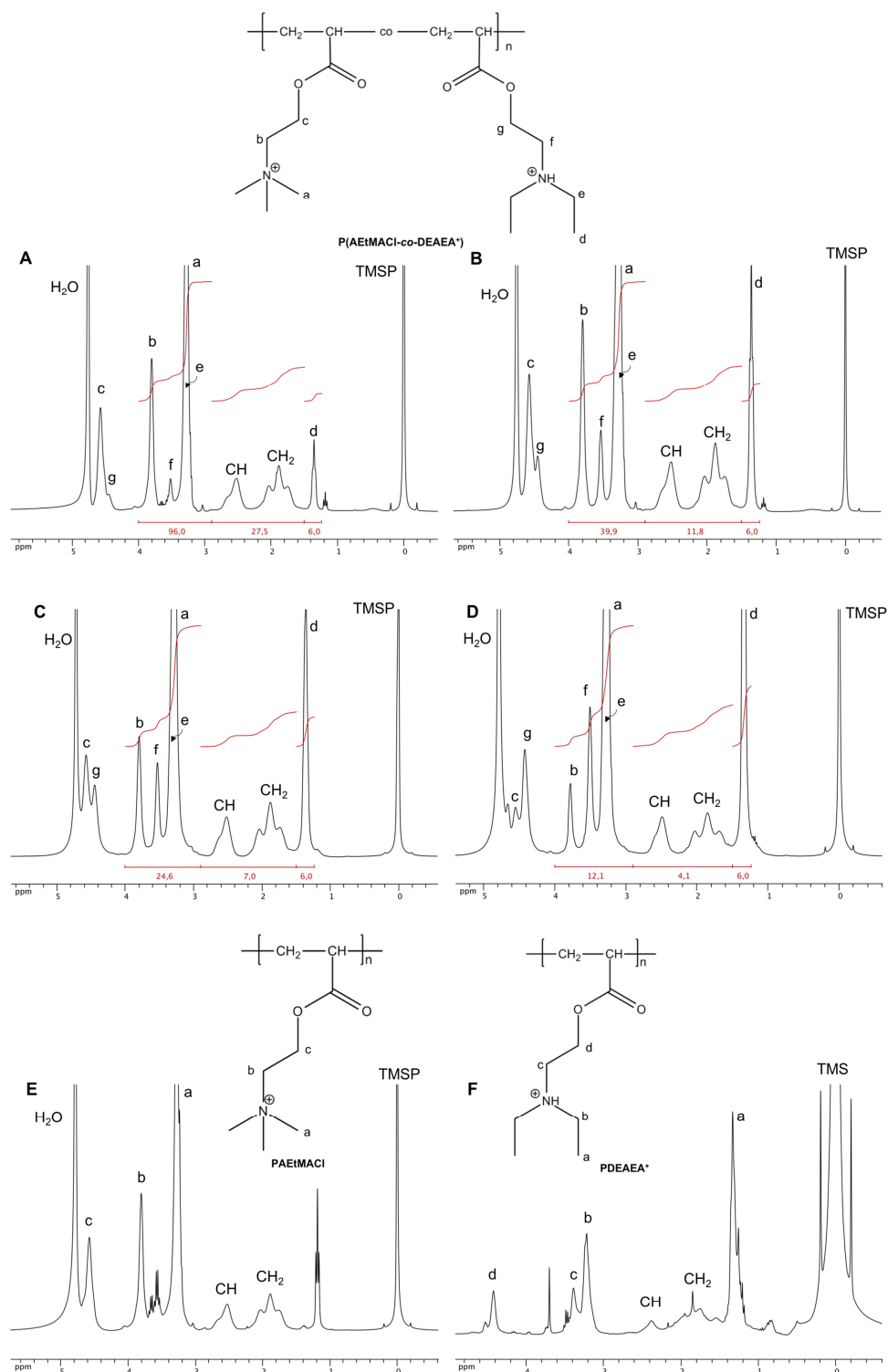


Figure S17. ^1H NMR spectra of precipitated $\text{P}(\text{AEtMACl-co-DEAEA}^+)$ copolymers in D_2O (A) 90/10 (Exp. 20), (B) 75/25 (Exp. 17), (C) 60/40 (Exp. 18), (D) 25/75 (Exp. 19), and homopolymers (E) PAEtMACl (Exp. 7) in D_2O and (F) PDEAEA⁺ (Exp. 12) in CDCl_3 . Letters correspond to proton attribution in the chemical structures.

8. (co)Polymer molecular weights

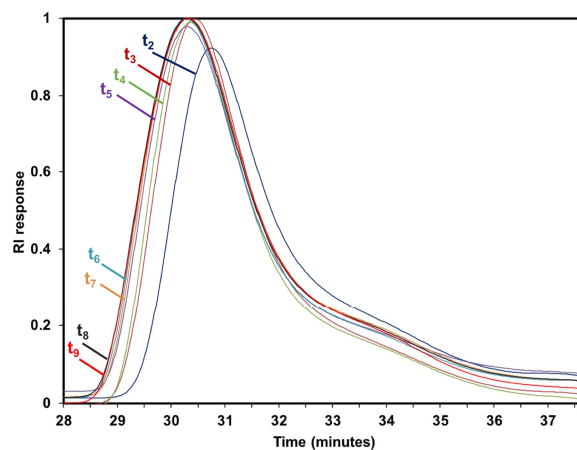


Figure S18. SEC chromatogram of copolymer P(AEtMACI-*co*-DEAEA⁺) 75/25 (Exp. 16) in acetate buffer, evidencing an unimodal molecular weight distribution.

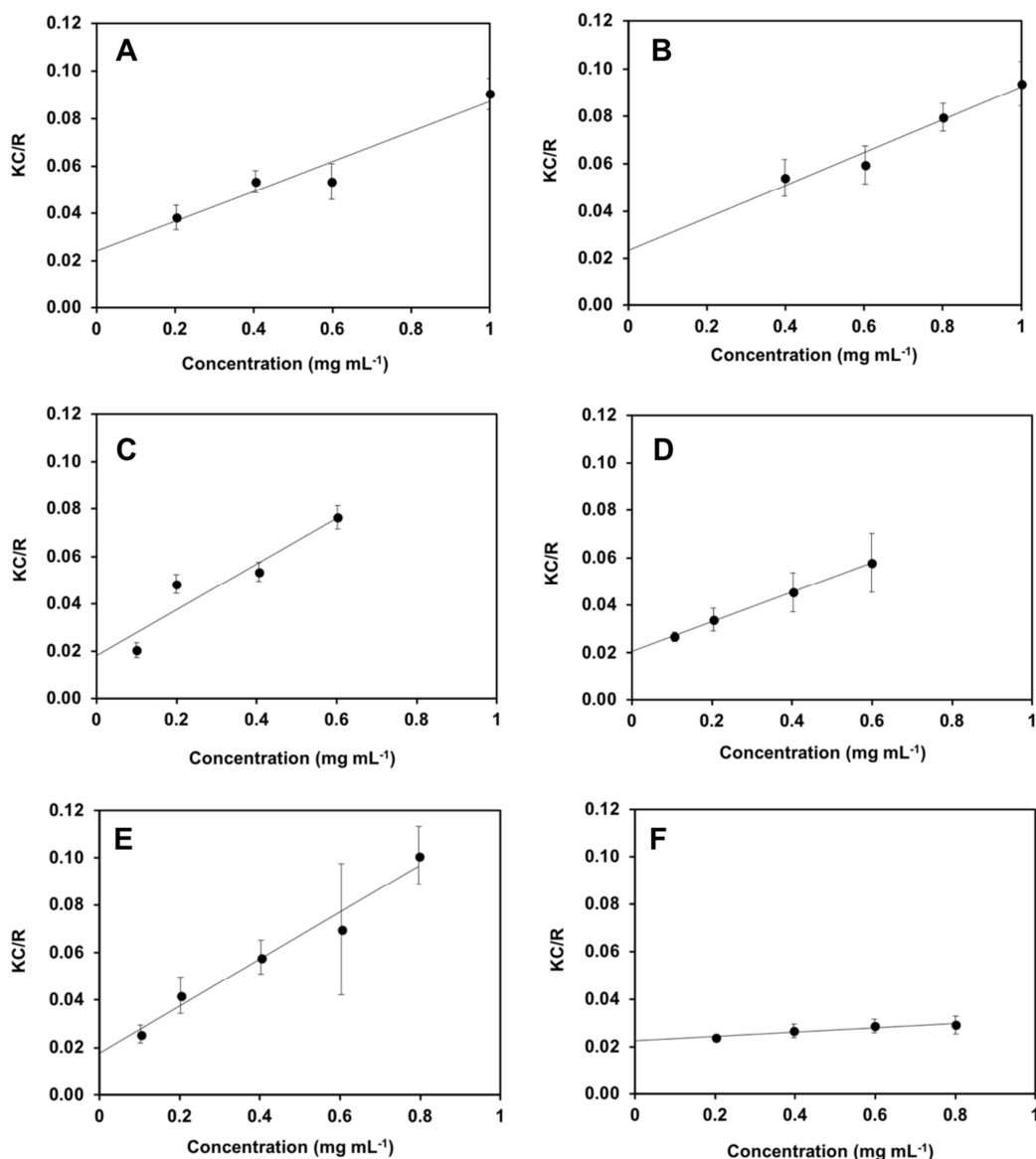


Figure S19. Debye plot (Static Light Scattering (SLS) measurements) for each polymer sample. (A) Exp. 12_{t10} (PDEAEA⁺) ($KC/R = 0.063 C + 0.0242$), (B) Exp. 8_{t7} (PAEtMACI) ($KC/R = 0.069 C + 0.0234$), (C) Exp. 17_{t7} (P(AEtMACI-co-DEAEA⁺) 75/25) ($KC/R = 0.096 C + 0.0183$), (D) Exp. 18_{t10} (P(AEtMACI-co-DEAEA⁺) 60/40) ($KC/R = 0.062 C + 0.0206$), (E) Exp. 20_{t8} (P(AEtMACI-co-DEAEA⁺) 90/10) ($KC/R = 0.099 C + 0.0176$), (F) Exp. 21_{t11} (P(AEtMACI-co-DEAEA⁺) 25/75) ($KC/R = 0.009 C + 0.0226$).

9. References

- ¹ F. D'Agosto, M.-T. Charreyre, L. Véron, M. F. Llauro, C. Pichot, *Macromol. Chem.*, 2001, **202**, 1689-1699.
- ² A. Laschewsky, M. Mertoglu, S. Kubowicz, A. F. Thiinemann, *Macromolecules*, 2006, **39**, 9337-9345.
- ³ M. Mertoglu, A. Laschewsky, K. Skrabania, C. Wieland, *Macromolecules*, 2005, **38**, 3601-3614.
- ⁴ G. Odian, *Principles of Polymerization*, Wiley-Interscience, New York, 4th ed., 2004.
- ⁵ H. Li, B. Han, J. Liu, L. Gao, Z. Hou, T. Jiang, Z. Liu, X. Zhang, J. He, *Chem. Eur. Journal*, 2002, **8**, 5593-5600.